

The impact of the January 15, 2010, annular solar eclipse on the equatorial and low latitude ionospheric densities

R. K. Choudhary,¹ J.-P. St.-Maurice,^{1,2} K. M. Ambili,¹ Surendra Sunda,³ and B. M. Pathan⁴

Received 25 January 2011; revised 10 June 2011; accepted 15 June 2011; published 14 September 2011.

[1] The January 15, 2010, solar annular eclipse crossed the magnetic equator in the middle of the day over India, in a region instrumented with several magnetometers, Total Electron Content stations using GPS data, and an ionosonde located very near the center of the eclipse. With the help of a one-dimensional model appropriate for the region of interest we show that the ionosonde data was consistent with a lower F region plasma that was moving upwards with only modest velocities in the morning hours and moving resolutely downwards in the afternoon hours. This motion agreed well with the local magnetometer data which revealed a weakened electrojet taking place in the morning hours while a full-blown counter-electrojet was present in the afternoon hours. We show that the unusual solar eclipse-induced electrodynamics resulted in a reduction in the Total Electron Content depletion not just at the magnetic equator but also, more markedly, in the Equatorial Ionization Anomaly (EIA) zone, a further 10 degrees to the north. This latter point clearly shows that the eclipse led to a cut-off in the supply of plasma provided through the equatorial fountain, by altering a fundamental aspect of the equatorial electrodynamics.

Citation: Choudhary, R. K., J.-P. St.-Maurice, K. M. Ambili, S. Sunda, and B. M. Pathan (2011), The impact of the January 15, 2010, annular solar eclipse on the equatorial and low latitude ionospheric densities, *J. Geophys. Res.*, *116*, A09309, doi:10.1029/2011JA016504.

1. Introduction

[2] For obvious reasons, the reduction in solar radiation during solar eclipses normally leads to ionospheric density depletion. Those changes are particularly easy to detect in the E region where chemical lifetimes are short owing to the dominance of molecular ions [Ratcliffe, 1956; Van Zandt *et al.*, 1960; Roble *et al.*, 1986]. They are far less straightforward in the F region where the chemical lifetime of the ions is so long that the densities can be affected by dynamical transport processes or even by gravity waves generated by the eclipse itself [Chimonas and Hines, 1970; Müller-Wodarg *et al.*, 1998; Altadill *et al.*, 2001]. Nonetheless, the ratio of uneclipsed to eclipsed electron density has been found to be of the order of 1.5 to 3.0 in the E-region and 2.4 to 3.6 in the F-region [Ratcliffe, 1956]. Satellite beacon measurements have also revealed decreases in total electron constant (TEC) in the ionosphere by a magnitude as high as 20–30% [Cohen, 1984; Afraimovich *et al.*, 1998]. Following

the passage of an eclipse, however, the electron densities recover their normal values.

[3] In a region like the magnetic equator, the impact of an eclipse can be more difficult to predict because wind systems create dynamos with currents that close in the equatorial electrojet (EEJ). Based on satellite observations, Tomás *et al.* [2007] have shown that eclipses can trigger a reversal in the EEJ (a counter-electrojet, or CEJ) at the magnetic equator and St.-Maurice *et al.* [2011] have proposed that ground-based observations can be explained by traveling low pressure centers associated with the center of the eclipse. Said low pressure systems would be responsible for a local reversal of the usual daytime wind patterns and would therefore trigger a CEJ. The dynamo-generated electric fields move the plasma vertically up under normal EEJ conditions (zonal electric field to the east) or down in CEJ conditions. Since gravity is nearly perpendicular to the magnetic field, the uplift or down ward motion of the plasma has a defining role on the plasma density profile. It follows that the equatorial densities should be affected by the special electrodynamics surrounding an eclipse straddling the magnetic equator. In turn, however, this should affect other latitudes through the so-called equatorial fountain effect [Hanson and Moffett, 1966; Anderson, 1973]. With a strong uplift (strong eastward electric field) the plasma is pushed upward and slides down to lower latitudes to feed the Equatorial Ionization Anomaly (EIA), typically 10 degrees poleward of the magnetic equator during the solar quiet conditions of interest

¹Space Physics Laboratory, VSSC, Trivandrum, India.

²Also at Institute for Space and Atmospheric Studies, University of Saskatchewan, Saskatoon, Saskatchewan, Canada.

³GAGAN, Airports Authority of India, Space Applications Centre, Ahmedabad, India.

⁴Indian Institute of Geomagnetism, Mumbai, India.

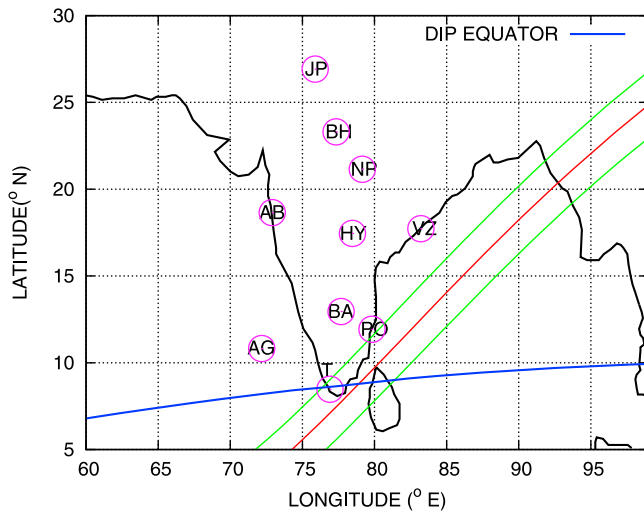


Figure 1. Totality path of the annular eclipse over the Indian subcontinent. Northern and southern limits of the antumbral shadow of moon shown by the green line, with red line showing the central position. Dip equator over the Indian region shown in blue. Locations of the stations from where the measurements were used also shown as letters symbols defined in Table 1.

in the present paper. Conversely, with a downward motion of the equatorial F region, the EIA should be cut off from its source. It follows that, since an eclipse is bound to affect E region wind patterns in the dynamo region outside the equator itself, it should, depending on the modifications that it induces in the winds and attendant current systems, have either a positive or negative impact on the plasma density distribution not just at the equator but well into surrounding latitudes through its effect on the vertical equatorial plasma drift.

[4] In an earlier publication dealing with the January 15, 2010, eclipse [St.-Maurice *et al.*, 2011] we have shown that a counter-electrojet (CEJ) was triggered by the eclipse in the afternoon sector and that the likely culprit was a low pressure center associated with the center of the eclipse. We also argued, based on ionosonde and magnetometer signatures, that the combination of the neutral wind pattern and conductivity gradients near the eclipse ‘terminators’ produced an accumulation of negative charges near each terminator akin to what is seen in the ‘Pre-reversal-enhancement’ of the

electric field often seen at sunset in the equatorial regions. We referred to this feature as a ‘double PRE’. In the present communication, we focus on a very different issue. We complement the original magnetogram and ionosonde data with the addition of other magnetometer data, Total Electron Content (TEC) values derived from GPS receivers, and model calculations from a one-dimensional model. We show from this extended data set that the Equatorial Ionization Anomaly (EIA) was not present on the day of the eclipse. From the model and the ionosonde observations, we also show that the equatorial lower F region plasma was moving upwards at reduced velocities in the morning and moving plainly downward for a large portion of the afternoon with the consequent result that the EIA was cut off from its equatorial latitude supply, thus explaining how it essentially disappeared on eclipse day.

2. Results

2.1. Eclipse Particulars and Observational Context

[5] The path of maximum obscurity for the annular solar eclipse of January 15, 2010 passed through the Indian Ocean. At its peak, the maximum duration of full annularity was observed for a little more than 11 min. Trivandrum (8.5°N, 76.9°E, 0.2°N dip-latitude) experienced a magnitude of 0.9216 at mid-eclipse with a 84.3% coverage of the sun’s disk. The First Contact of the shadow of the moon at Trivandrum was at 11:05 IST, or 6:35 UT. (Local Time, LT, at Trivandrum = IST – 22 min). Maximum obscuration started at 13:10 IST and lasted until 13:18 IST with mid eclipse at 13:14 IST. Over Trivandrum, the event ended at 15:07 IST.

[6] In Figure 1, we display the path of the eclipse over the Indian subcontinent. The path of totality is centered between the two green lines, showing the northern and southern limits of the antumbral shadow. The red line shows the central path while the line in blue represents the dip equator. Also shown in Figure 1 are the locations of stations housing different instruments used in this study. Table 1 provides further details about the notations used for the different stations, their instruments, and the geographic and geomagnetic locations, the percentage obscurity of the sun that was attained during the eclipse, and the difference between IST and LT at those stations.

[7] The eclipse took place during a magnetically quiet period consistent with the very quiet solar wind at the time. Only minor variations (less than 10 nT in magnitude) were

Table 1. Details on the Locations of Different Stations and Instruments Therein Used in the Present Study

Symbol	Station	Geographic Latitude	Geographic Longitude	Geo-magnetic Latitude	Geo-magnetic Latitude	Instrument	% Obscurity	IST - LT (min)
T(R)	Trivandrum	08.47°N	76.92°E	00.17°S	149.54°E	Digisonde/GPS	84.3	22
T(I)	Tirunelveli	08.77°N	77.82°E	00.40°N	150.42°E	Magnetometer	84.3	19
AG	Agati	10.51°N	72.11°E	02.36°N	144.98°E	GPS	71.9	42
PO	Pondicherry	11.93°N	79.83°E	03.00°N	152.72°E	Magnetometer	83.2	11
BA	Bangalore	12.95°N	77.68°E	04.19°N	150.64°E	GPS	77.1	19
VI	Vizag	17.72°N	83.23°E	08.49°N	156.40°E	GPS/Magnetometer	76.8	-3
HY	Hyderabad	17.45°N	78.47°E	08.58°N	151.80°E	GPS	67.5	16
BH	Bhopal	23.28°N	77.34°E	14.47°N	151.24°E	GPS	51.6	21
AB	Alibagh	18.64°N	72.91°E	10.26°N	146.57°E	Magnetometer	53.6	38
NP	Nagpur	21.15°N	79.15°E	12.19° N	152.77°E	Magnetometer	60.2	13
JP	Jaipur	26.92°N	75.89°E	18.17°N	150.19°E	Magnetometer	41.2	26

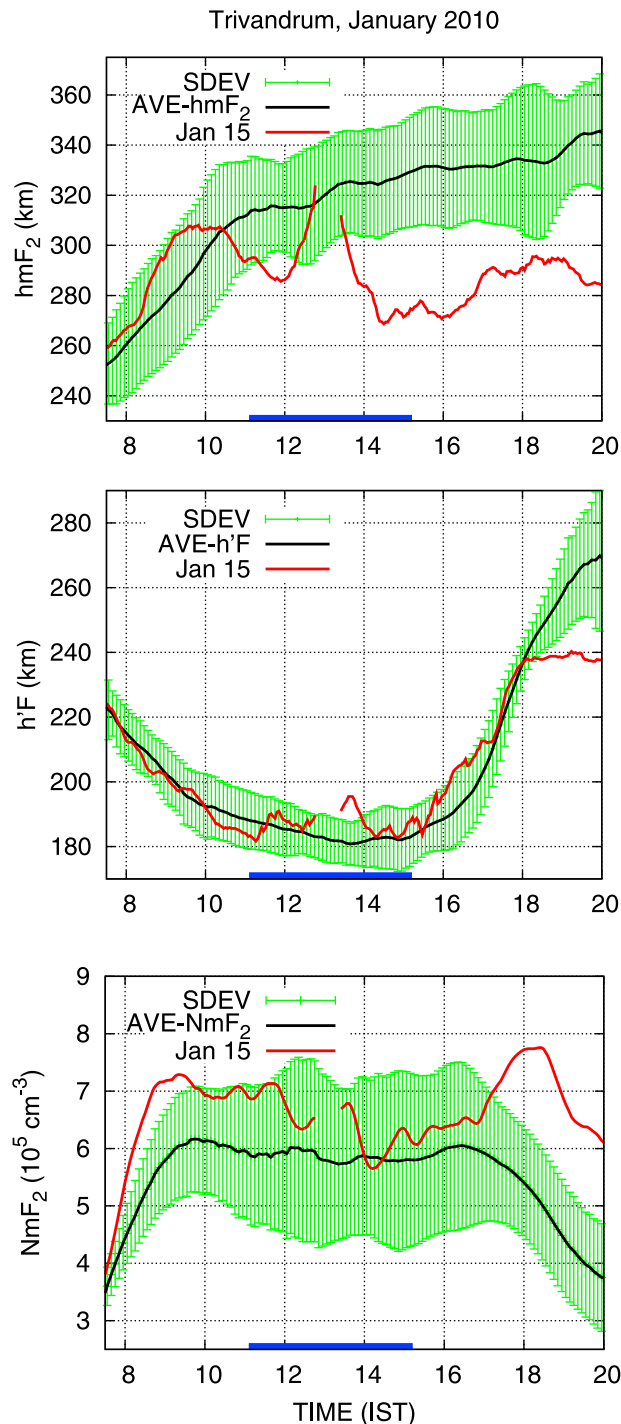


Figure 2. Temporal variations in (top) hmF_2 , (middle) $h'F$ and (bottom) NmF_2 on eclipse day (January 15) and their comparison with their monthly average and their standard deviations recorded from the digital ionosonde in Trivandrum in January, 2010. Thick blue bar along the X-axis: time interval during which there Trivandrum was eclipsed.

observed in the Dst index between January 13 and January 16, 2010. There were nevertheless a few periods of weak to moderate substorm activity in the days that led to the period of interest. The noteworthy activity on January 14 consisted of only one episode during which the AL was between -200

and -250 nT for two hours during 11 UT and 15 UT. Given the lack of storm activity as such, the high latitude magnetic activity could influence the lower latitude electrodynamics only through a disturbance dynamo triggered by a substorm [Blanc and Richmond, 1980]. On January 14, the Tirunelveli magnetometer data did indeed indicate that substorm activity from the day before (AL between -200 and -400 nT for five continuous hours on January 13) resulted in horizontal magnetic field fluctuations smaller than the January average by 35 nT, around 14 LT. However, on January 15, the departures from the average were by an additional 15 nT in spite of the much weaker substorm activity on the previous day. This provided a strong indication that the eclipse had an important impact on the equatorial electrodynamics, which is in general agreement with the previous equatorial eclipse observations [e.g., Tomás *et al.*, 2007].

2.2. Ionosonde Data

[8] We have used Digital Ionosonde measurements (Digisonde -DPS4D) at Trivandrum ($8.47^\circ N$, $76.92^\circ E$, $0.17^\circ S$ dip-latitude) to retrieve electron density profile information. The DPS-4D Digisonde is an advanced digital ionospheric high frequency pulse sounding system developed at the University of Massachusetts Lowell's Center for Atmospheric Research (UMLCAR). It sweeps frequencies in the range 1–30 MHz and provides reliable estimates for the electron density, at least below the F2 peak. The electron density profiles are derived using the true height inversion algorithm embedded in the SAO Explorer software package (<http://umlcar.uml.edu/SAO-X/SAO-X.html>). Details on the estimation of electron density profile from Digisonde measurements are given by Reinisch and Huang [2001] and Kutiev *et al.* [2009]. Digisonde-derived electron density profiles have been used extensively in the study of various solar-terrestrial phenomena [Lee and Reinisch, 2007; Zong *et al.*, 2010]. This stated, given the very low latitude involved and the special conditions prevailing during the eclipse, we have refrained from using any density estimation derived by the software algorithm above the F2 peak, since such estimates are based on empirical information, e.g., the IRI model.

[9] The salient features of the regional ionospheric consequences of the eclipse are illustrated in Figure 2 through a presentation of various digisonde-derived parameters on the day of the eclipse. A comparison is made with their average and their standard deviation obtained for January 2010. In Figure 2 (top) we present the height of the F region peak (hmF_2) observed at Trivandrum on January 15. For the calculation of the monthly average, we considered the data set for the entire month except for the eclipse day (January 15) and five universally identified magnetically disturbed days for that particular month (January 11, 13, 20, 21, and 30).

[10] It is clear from Figure 2 that, on average, the hmF_2 quickly rises from 250 km around 7:00 Indian Standard time (IST) to approximately 310 km altitude in the afternoon ($\sim 11:30$ IST). It rises more slowly but steadily thereafter and reaches a height as high as 350 km by 20:00 IST, well after sunset. Figure 2 (middle) shows the height of the bottom side of the F-region ($h'F$). We note a steep increase in $h'F$ from about 220 km at 18:00 (a normal local sunset time) to 270 km by 20:00 IST, indicative of a frequently observed 'pre-reversal electric field enhancement' (PRE) near the

evening terminator [Farley et al., 1986; Rishbeth, 1971; Eccles, 1998]. Figure 2 (bottom) describes the variations in the density at the F2 peak (NmF2).

[11] Figure 2 clearly shows that after having reached a normal (for that time of year) peak value of 310 km at 10:00 IST, the hmF2 behavior on the day of the eclipse (January 15, 2010) diverged from its monthly mean, moving resolutely down after 10:00 IST. This was unusual in the sense that it indicated a decrease, and possibly a change in sign, in the uplift rate, and, by inference, in the zonal electric field that was lifting the plasma up. While the time taken to reach 310 km has to vary from day to day (since it depends on the strength of the zonal electric field), a decrease in the electric field this early in the morning was unusual. In addition, the 10:00 IST descent was followed later on by another unusual signature, namely, an up and down oscillation shortly after noon, which we have previously discussed at length [St.-Maurice et al., 2011]; we argued that there was an accumulation of negative charges near the eclipse ‘terminators’, the latter being highly reminiscent of a double “Pre-reversal Enhancement” (PRE) signature in the electric field. We showed that the double PRE could be explained using a mechanism initially proposed by Farley et al. [1986]. We note that Sridharan et al. [2002] had similarly reported an enhanced PRE at Trivandrum during the eclipse of August 1999 as it was entering the sunset terminator region. Sridharan et al. [2002] evaluated the role of F-region dynamo triggered either by the curl-free nature of the electric field near the sunset terminator [Rishbeth, 1971; Eccles, 1998] or the Farley et al. [1986] mechanism and concluded that both mechanisms were needed to explain the observations.

[12] Aside from the terminator-induced oscillation which we will not discuss any further, the most noticeable feature in the hmF2 on eclipse day was its abnormally low altitude, particularly between 1400 and 1600 IST. This was followed by a partial recovery, which suggested a plasma uplift due to a resurgence in the eastward zonal electric field. However, Figure 2 also shows that the hmF2 could not recover its normal value even by 2000 IST.

[13] No doubt in relation to the abnormal behavior in the hmF2, the most unusual feature in the behavior of the F peak plasma density (NmF2, shown in Figure 2 (bottom)) was its notably high value after sunset, at a time when it should have been receding. Given that the height of the F-region peak was abnormally low around that time (Figures 2 (top) and 2 (middle)), this indicates that the lower F region plasma could, as a result, not be transported up and, therefore, it stagnated at lower heights than usual. The layer was then compressed compared to normal days and therefore ended up with a higher plasma density near the peak (more on this below).

2.3. Magnetic Field Data

2.3.1. The Removal of Global Scale Magnetic Perturbations

[14] The magnetic field fluctuations that are recorded by ground-based magnetometers contain contributions both from the local magnetic field variations, and the global field fluctuations associated with ring currents (*Dst* or *SYM-H*) [Rastogi and Klobuchar, 1990; Le Huy and Amory-Mazaudier, 2005]. Several procedures could be taken to

isolate the local fluctuations from the global one. If one were to solely isolate the EEJ contributions, one approach introduced by Nair et al. [1970] and later used by Rastogi and Klobuchar [1990], and which works well under ordinary circumstances, is to subtract the ΔH values from a low latitude station like Alibagh from those at Tirunelveli. This method assumes that the connection between the Sq current perturbations at Alibagh and the EEJ current at Tirunelveli does not change from day to day so that subtracting one from the other removes the global contributions that modulate both records in the same way. The drawback of this approach is that when the Sq current system is perturbed by unusual winds during an eclipse or a disturbance dynamo day, the relation between the Alibagh perturbations and the EEJ perturbations should easily deviate from the norm. We therefore adopted a different approach for our study of the eclipse.

[15] In an earlier approach [St.-Maurice et al., 2011] we subtracted the 2 AM data of a given station from its instantaneous value during the day. This was possible because January 15 was a magnetically quiet day, with less than a 10 nT variation in the *Dst* index during the course of the day. Still, while this method allowed us to produce a reasonable estimate over the magnetic fluctuations at the equator, where the perturbations are relatively strong, it turned out to be increasingly inaccurate as we moved away from the equator and had smaller magnetic fluctuations to deal with.

[16] In the present work we used yet another approach wherein we took advantage of the availability of the *SYM-H* index to remove global contributions from individual stations. This removed the need to use Alibagh to take out the global current contributions from the equatorial magnetograms so that if something unusual was happening in the Sq current system, it would not introduce erroneous interpretations in the magnetic fluctuations induced by the equatorial electrojet.

[17] We took an empirical approach to assess how the global currents responsible for the *SYM-H* variations affected individual stations. To that goal, we first studied the local magnetic fluctuations at a time when local contributions should be minimal, namely, we produced a linear regression between the local perturbations and the *SYM-H* variations for the month during the local time interval 2 AM to 3 AM. This gave us the average response of a station for the month, which we labeled as H_{symH}^m and were able to describe through the equation

$$H_{symH}^m = H_0 + C \times SymH \quad (1)$$

where the background magnetic field H_0 and the constant C were obtained from a linear regression mentioned above. Under normal circumstances the perturbation from local currents, ΔH_{local} , could be obtained by removing the *SYM-H* contribution using

$$\Delta H_{local} = H_{obs} - H_0 - C \times SymH \quad (2)$$

where H_{obs} was the observed magnetic field at any given time while $SymH$ was obtained from the recorded value at the same particular time, with H_0 and C for the station at hand. However, we added one more step to the procedure to account for possible systematic drifts in the instruments or in the *SYM-H* index determination on a multi-day basis. These

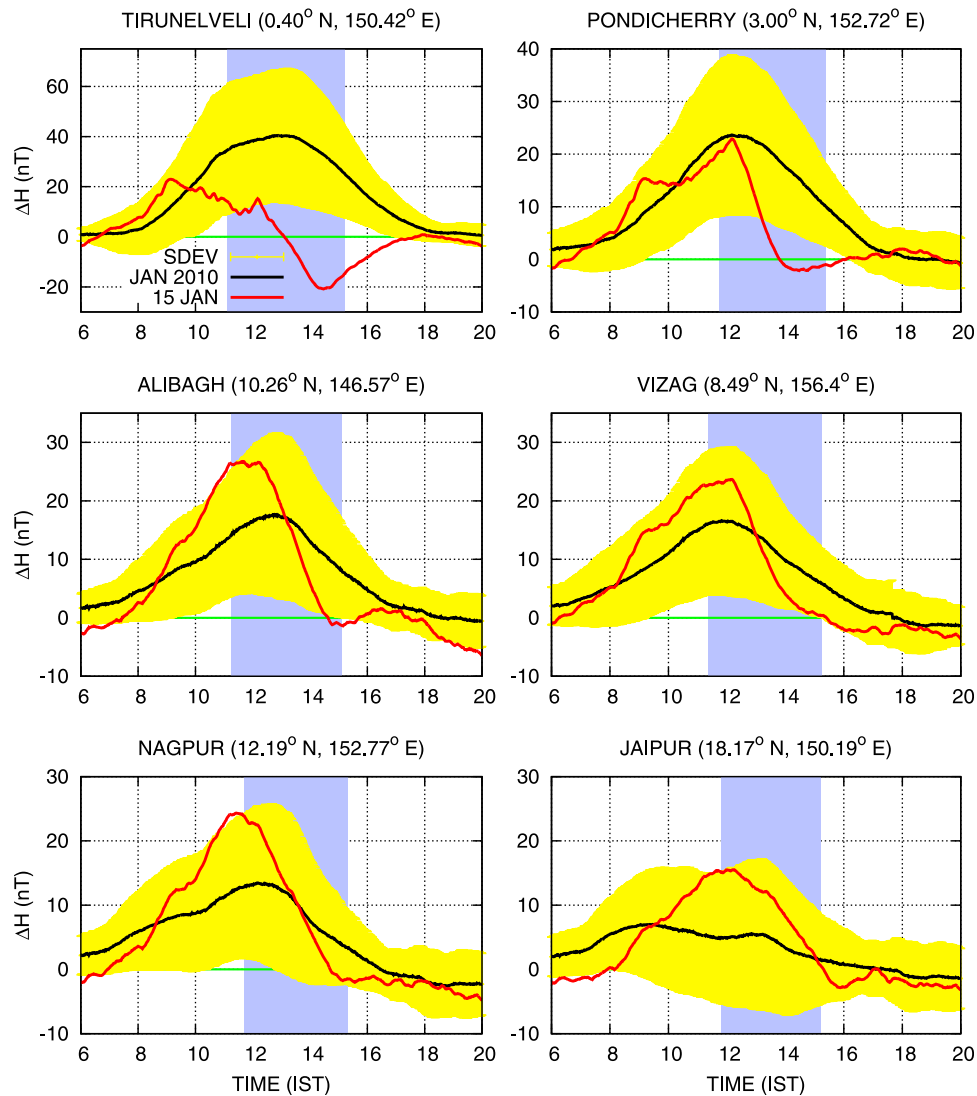


Figure 3. Monthly average of ΔH (black lines) and one σ deviations from the average (yellow area) observed at six low latitude stations in India during January, 2010. Red lines: ΔH for January 15, 2010. Data for the eclipse day and five disturbed days (January 11, 13, 20, 21, and 30, 2010) were excluded from the statistics. Highlighted blue regions indicate the duration of eclipse at each station.

effects would be equivalent to having a small but not entirely negligible variation in the value of H_0 from one part of a month to another, while the proportionality constant C would not change. To account for this possibility we subtracted the 2 to 3 AM average value of H_{SymH} for the day from its instantaneous value obtained later during the day. We did the same for the observed value of H , namely, we subtracted the averaged 2 to 3 AM value from the instantaneous value. Our final determination of ΔH for a given station was therefore given by

$$\Delta H = (H_{obs} - H_{2-3AM}) - C \times [SymH - SymH_{2-3AM}] \quad (3)$$

It is important to note that this method would only give a different result from equation (2) if H_0 were to differ from its monthly average on a particular day.

[18] It should be noted that there is still a caveat to this third method: for $SymH$ estimates, the four most quiet days

of the month are taken together and averaged in order to empirically obtain the contributions from the Sq current for that month. This means that when we use the $SymH$ during anomalous Sq current conditions, the corrections used for the Sq cannot be quite right. For example, supposing there is a strong CEJ (counter electrojet) on a day under study (as seems to be the case on eclipse day), the contribution from the Sq would have been overestimated for that day, meaning that the $SymH$ would have itself been underestimated, so that the background removal would not have been quite large enough. Still, this is the best we can do under the circumstances. This caveat must simply be kept in mind.

2.3.2. Magnetic Fluctuations at the Indian Stations

[19] In Figure 3, we show the ΔH variations recovered from our $SymH + H_0$ removal procedure. We present data from magnetograms located at six different Indian stations. The stations cover a range of geomagnetic locations, from

equatorial (Tirunelveli), to near equatorial (Pondicherry), and low latitude (Vizag, Alibagh, Nagpur, and Jaipur). The geomagnetic coordinates of the stations are mentioned in bracket at the top of each panel and their locations are also presented in Figure 1. Highlighted blue regions indicate when the eclipse passed through those stations. At the equator, we used the magnetic data from Tirunelveli instead of Trivandrum, as the former is the standard geomagnetic observatory and is located nearby, 81 km to the magnetic east of Trivandrum.

[20] We can see in Figure 3 that, at first, the January 15 magnetic field perturbations (ΔH) increased steadily at all stations, in line with the average trend, although a bit faster than average (although this was the case for that particular week). However, at the dip equator (Tirunelveli), after 9:00 IST, the current started to weaken and became progressively smaller until the noon hour, when the first part of the ‘double PRE’ referred to in the introduction introduced a brief increase in the electric field. By then the ΔH was about 20 nT, or 20 nT less than normal for that time of day. The decrease continued until a full-fledged counter electrojet (CEJ) ensued reaching down to -20 nT shortly before 15:00 IST, after which a gradual recovery to normal values by 18:00 IST.

[21] Pondicherry (3.0°N Dip Latitude) had a similar behavior to Tirunelveli except for the fact that the magnitudes involved were smaller, as should be expected from a station somewhat north of the magnetic equator, where the EEJ is no longer very intense. One important distinction is that the sign of the currents at Pondicherry came close to zero but never flipped, at least according to our subtraction methodology. We come back to this question in section 3.

[22] Moving from the dip equator towards the anomaly zone, one can see that there was no hint of weakening in the zonal current after 09:00 IST at the equator. On the contrary, the magnetic perturbation ΔH became larger than normal, by as much as 20 nT above the standard deviation even by 18° to the magnetic north, well past the crest in the equatorial ionization anomaly.

[23] Finally, after 12:15 IST, a sharp decrease in currents was evident at all stations so that by 15:00 IST all stations poleward of 3° had come back down to normal values (i.e., within one standard deviation) for that time of day, while by the same time the equator reached its largest negative current values. Things stayed relatively close to the normal from that point on, at least poleward of Pondicherry.

[24] We stress that the enhancement in the morning low latitude currents and the afternoon CEJ observed near the dip equator on eclipse day were both clearly anomalous. Furthermore, as already described in section 2.1, there was no magnetic activity until late on January 15, 2010 so that these signatures could not be due to a prompt penetration electric field [Fejer and Scherliess, 1997]. In addition, as also described in section 2.1, there was only a weak magnetic substorm on the day before the eclipse, making it unlikely that there could have been a strong disturbance dynamo [Blanc and Richmond, 1980; Le Huy and Amory-Mazaudier, 2005] on the day of the eclipse. The most likely factor left to explain the presence of the anomalous features therefore had to be the eclipse itself.

2.4. Total Electron Content Data

[25] In Figure 4 we show the evolution of the GPS-derived Vertical Total Electron Content (VTEC) of the ionosphere over the Indian equatorial and low latitude regions for January 15, 2010. Once again, we compare with the monthly average and one standard deviation for the whole month of January 2010. The VTEC was estimated using a standard technique described by Smith *et al.* [2008]. To generate the statistics we considered measurements at any receiving station if VTEC measurements pertained to an ionospheric region within ± 1.5 degree latitude/longitude of the station.

[26] The geographic and geomagnetic coordinates of the GPS stations used in this study are given in Table 1. Two of the stations (Trivandrum, and Agati) are very close to the magnetic equator and fall in the Equatorial Electrojet (EEJ) belt, being at 0.2°S , and 1.2°N , geomagnetic latitude respectively. The Bangalore station, being at 4.1°N Dip latitude, is just outside the EEJ belt. By contrast, the other three stations, namely, Vizag (8.6°N), Hyderabad (8.8°N), and Bhopal (14.2°N geomagnetic latitudes) are located in the vicinity of the equatorial anomaly zone (which can reach geographic latitudes as high as 25°N during high solar active periods). Under periods of low solar activity, as with the year 2010, the anomaly crest, on average, saddles somewhere near the Hyderabad Latitude. Finally, Table 1 also shows the % obscuration of the sun’s disk at each stations recorded during the eclipse event on January 15, 2010. The highlighted blue regions in the Figure 4 mark the time at which the solar eclipse overlaps with each station. The VTEC measurements presented in this study were obtained under the GAGAN (GPS Aided Geo Augmented Navigation System) program.

[27] A first noticeable feature from Figure 4 is that the VTEC for all the stations during and after the eclipse was low compared to the mean plus standard deviation. At Trivandrum, we only had measurements after 12:50 IST on January 15, but we still could see an appreciable depression in VTEC during the period of the eclipse, as compared with the monthly averages and their standard deviations.

[28] Interestingly, all the stations between 2 and 10°N dip latitude reached a maximum VTEC by 10:00 IST that was of the order of one standard deviation or more above the normal value for the month for that time of day. After that initial peak, however, all stations, including the equatorial one, ended up from noon onwards with a substantial VTEC reduction, with a value well below one standard deviation from the mean for the month. Thus, the VTEC became abnormally low on eclipse day, particularly following the passage of the eclipse over the region.

[29] The VTEC value at the equatorial stations went back to normal by sunset, at 18:00 IST. On the other hand, for stations farther away from the equator, like Hyderabad, the VTEC depletion was larger and never recovered, even by 20:00 IST.

3. Discussion

[30] We have shown in the previous section that the VTEC was reduced at all latitudes including the equatorial region. We have also seen that the ionosonde and electrojet

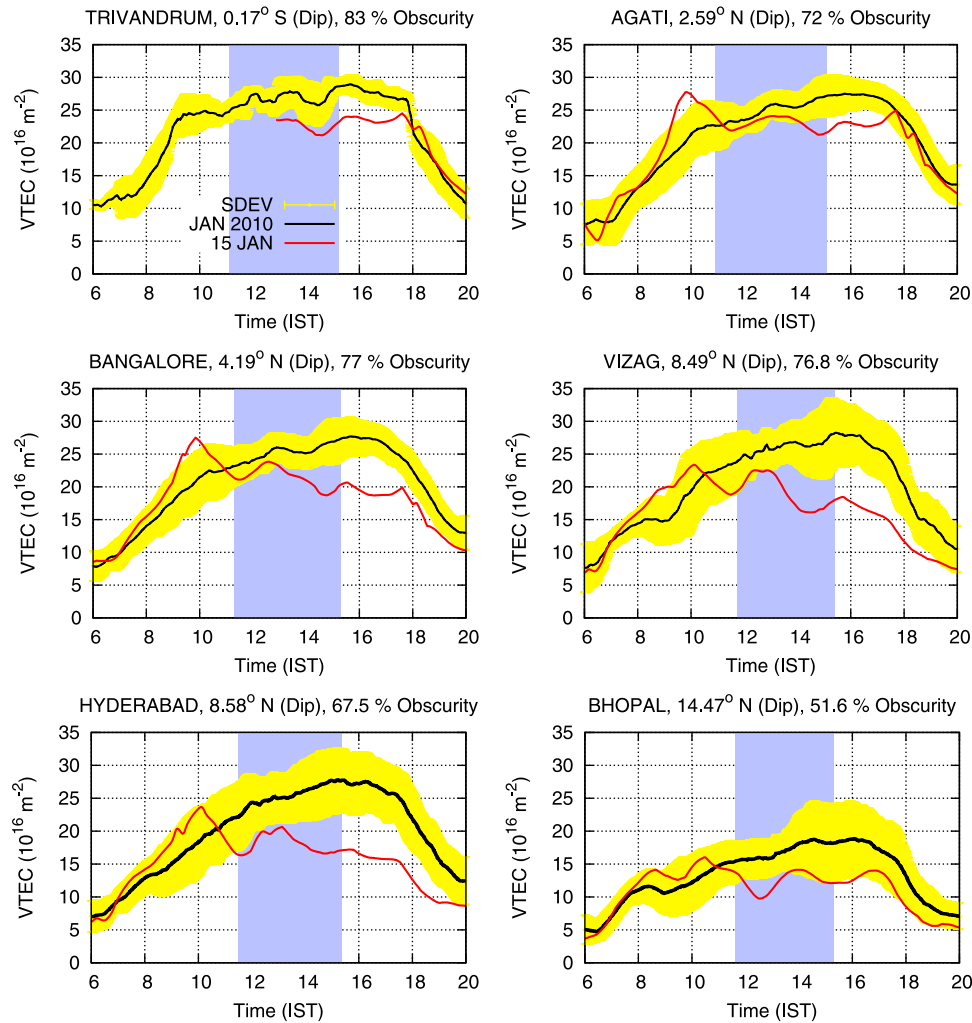


Figure 4. Temporal variation of VTEC at four Indian GPS stations between 0600 and 2000 IST on January 15, 2010. Also shown are the monthly TEC average for January 2010 along with its standard deviation. Highlighted blue regions represent the time interval for the eclipse at each station.

data both indicated that the zonal electric field in the E and lower F regions not only weakened but even reversed its sign, causing the plasma to drift weakly upward or just plain downward for an extended period of time. In the present section we argue that this cut off the supply of plasma to the upper F region, implying that the Equatorial Ionization Anomaly (EIA) was not fed as much as usual, if at all, through the equatorial fountain effect.

3.1. Quantitative Assessment of the F Region Dynamics

[31] The equatorial fountain effect is only effective if the F region plasma reaches 700 km altitude or above in large enough quantity [Anderson, 1973; Greenspan *et al.*, 1991]. To assess how much plasma could have been going up to higher altitudes, we numerically solved the one-dimensional continuity equation [Kelley, 1989]. We included the standard F region chemistry [St.-Maurice and Torr, 1978; Schunk and Nagy, 2000] i.e. photoionization, conversion of O^+ ions into molecular ions, dissociative recombination of the latter, and vertical advection from the vertical component of the plasma drift associated with the zonal electric field and the resulting $\mathbf{E} \times \mathbf{B}$ drift. We used horizontal

magnetic field lines and therefore did not consider the effects of gravity. For our initial conditions we assumed that the plasma density at sunrise was negligible, based on the ionosonde observations. Finally, in view of the observation of simultaneous positive electrojet currents and F region downward motions, we considered situations where the vertical drift could either increase or decrease with altitude or simply remained altitude-independent. The various aspects of the model are highlighted in the form of a block diagram in Figure 5.

[32] We used the 1-D model in order to extract vertical drift information from the digisonde densities. These densities are reproduced in Figure 6 (top), taken from Figure 1a of St.-Maurice *et al.* [2011] which displays the range-time density map on January 15, 2010 retrieved from the Trivandrum digisonde. Note that this is the data that was used to plot the hmF2 and NmF2 in Figure 2. An important point to stress again here is that, in principle, an ionosonde cannot give information above the F peak. This is why we did not use the digisonde density reconstructions to compute a TEC (Ionospheric Total Electron Content) value. It is also the reason why density differences above the F peak between

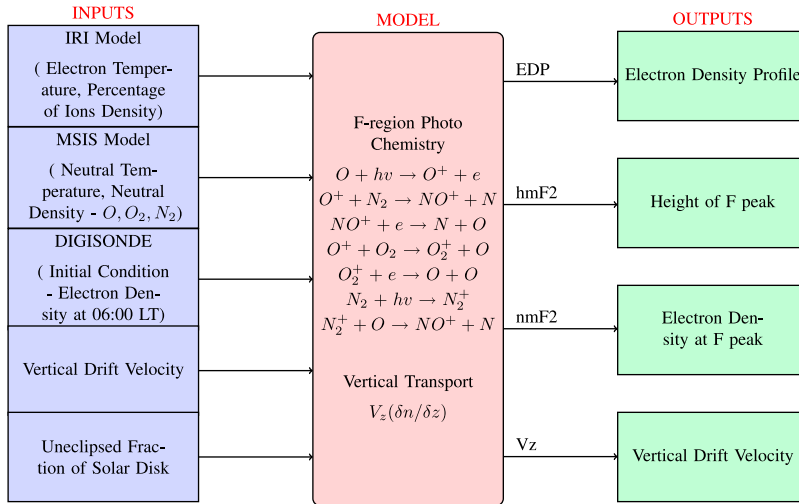


Figure 5. Block diagram for the one-dimensional model used in the present work.

computations and reconstructed digisonde densities should be ignored. In other words, the density profiles reconstructed from the ionosonde data only serve a qualitative purpose above the F peak.

[33] Since the reconstructed digisonde densities could not be relied upon above the F peak, we used our 1-D model primarily to reconstruct the F region peak position and density without worrying about matching the densities to the

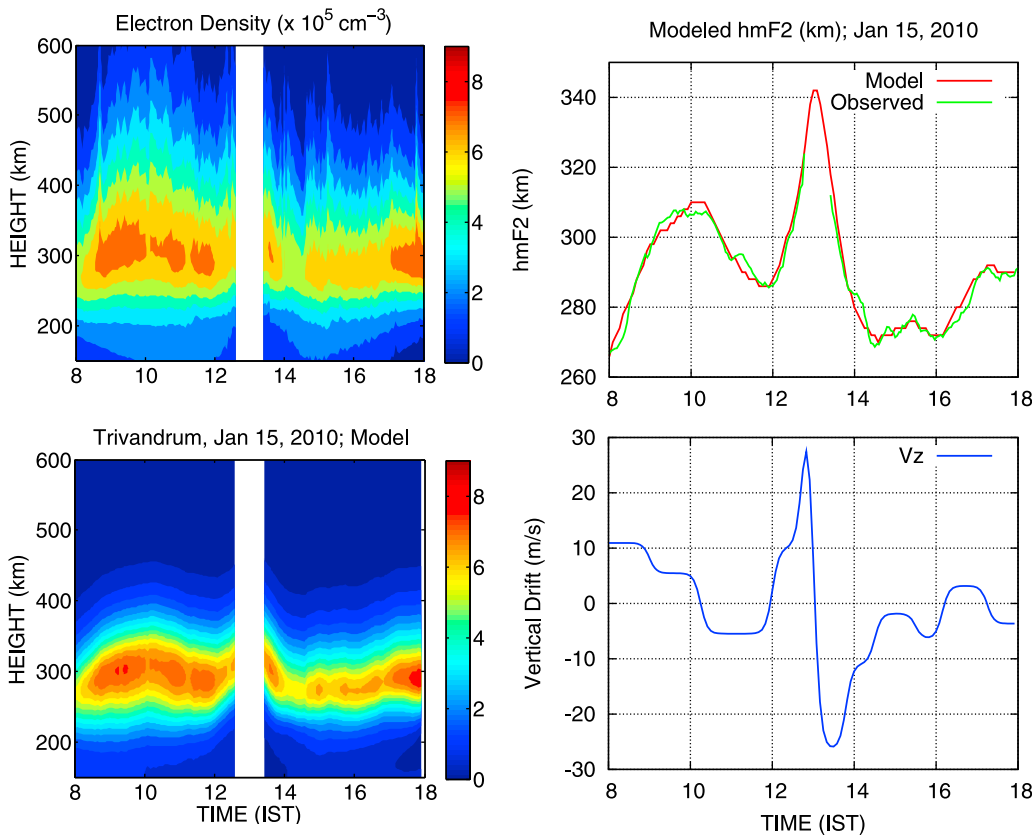


Figure 6. (top left) Range-time density maps deduced from the Trivandrum digisonde data on January 15, 2010 [after *St.-Maurice et al.*, 2011]. (bottom left) Range-time density maps obtained from numerical calculations where the vertical drift was adjusted as a function of time so as to have the modeled hmF2 match the observed value. (top right) A comparison between the hmF2 that were reproduced by the calculations and those that came from the observations. (bottom right) Vertical drift values retrieved from the model calculations.

digisonde-reconstructed densities above the F peak. However, having calibrated the photoproduction rates to reproduce the densities in chemical equilibrium regions below 200 km altitude, the only other parameter that we could use to reconstruct the F region peak was the vertical drift. The model electron density profiles that we produced by adjusting the vertical drift in order to fit the F peak position are given in Figure 6 (bottom left). In Figure 6 (top right) we show that the hmF2 observations could be fitted to near-perfection with the model.

[34] As far as the densities themselves were concerned, the observed densities were not reproduced well by the calculations in the earlier part of the morning. However, they were reproduced reasonably well later on. We could only attribute the early morning differences (in densities, not height) to a zonal electric field that would vary significantly with altitude or to a divergence in the meridional wind blowing along the magnetic field lines. Note that a meridional wind divergence along the magnetic field could have been produced by horizontal wind shears that were neither purely meridional nor purely zonal [Reddy and Devasia, 1973]. However, introducing such features was besides the point of our study and therefore beyond the scope of our model.

[35] The main motivation for the construction of the numerical model was to determine the direction and magnitude of the equatorial plasma drift near the F peak around the eclipse time. The drift that we found was needed to explain the behavior of the F peak is shown in Figure 6 (bottom right). For this particular calculation we used a uniform drift and were able to obtain an excellent fit to the density, including the NmF2 and hmF2 at all times after 10:00 IST. We could also obtain a high quality fit to these parameters before 10:00 IST by letting the vertical drift be altitude dependent between 200 km and the F peak.

[36] The model calculations were used in order primarily to determine the rate of ascension or of downward motion of the F peak. This motion could not be determined from a derivative of the F peak position with respect to time since the latter does not match the plasma drift when chemistry plays a role in the determination of the density. Two central results emerged from our analysis: (1) the plasma was moving down between 10:00 and 12:00 IST even though the electrojet current was still clearly positive. This inference requires some further discussion and is the topic of section 3.2; (2) according to the calculations, very little plasma made it even to 400 km altitude during the day of the eclipse.

[37] It is reasonable to assume that the EIA was weak to non-existent on eclipse day, particularly in the afternoon, because little plasma made it above 400 km altitude. Indeed, our model calculations indicate that, in order to explain the ionosonde observations at and below the F peak, the plasma actually had to be moving down for most of the afternoon. The physics that led us to this conclusion works as follows: above 300 km, the recombination rate is small since the density of molecular neutrals is small. Furthermore, even though the photo-production rate decreases exponentially with height, the presence of production with little recombination would cause the net plasma density above 300 km to increase throughout the day (a steady state is reached only if the plasma density exceeds 10^{13} m^{-3} , which is never observed and would indeed require much longer than the

roughly 12 hours of sunlight than there are in a day). Thus, in the absence of any vertical motion, the plasma would accumulate around 300 km for the solar conditions prevailing at the time of the eclipse. Now consider a positive vertical motion: in that case, the plasma spreads upward away from the region of maximum production, since the plasma moves away from the source region. The result is an F region peak that is advected upward, with the caveat that the motion of the F peak is slower than that of the plasma drift itself, because of chemistry. This is true particularly if the peak happens to be below 300 km altitude. Thus, as a result of the upward motion and the chemistry, the plasma spreads out, the F peak moves upward, and the NmF2 decreases. Moreover, in the absence of a substantial overall removal by the equatorial fountain effect, the VTEC would have to increase, given the reduction in the overall plasma recombination rate due to the plasma motion away from molecular neutrals.

[38] Consider next the opposite situation of a downward plasma drift: all the way down to 150 km altitude, the plasma moves towards a region of increasing production rate. This, by itself increases the plasma density everywhere, including near the F peak. However, the neutral density also increases with decreasing altitude, which means that the O^+ ions, below 250 km altitude in particular, are converted to molecular ions at an increasing rate. As a result, the dissociative recombination rate increases and the overall plasma density has to go down. Therefore, the plasma density increases at the F peak, even though the overall column plasma density registered by a VTEC observation actually goes down.

[39] In summary, our modeling of the digisonde observations confirms that the F region plasma was not feeding the EIA after 10:00 IST, because the drift was predominantly downward except for the one hour during which a PRE was observed near the noon hour terminator induced by the eclipse. Our model calculation shows that one hour was inadequate to push enough plasma above 400 km altitude in comparison to a sustained upward drift of 20 m/s or more lasting for several hours (not shown). With predominantly negative vertical motions for the rest of the time, there was therefore simply no way to feed the EIA on January 15, 2010.

3.2. Downward F Region Plasma Drift During a Weakened EEJ

[40] As mentioned above, Figure 6 (bottom) shows that the vertical plasma drift at 300 km had to be downward between 10:00 and 12:00 IST if we are to reproduce the salient features of the observations through our simulations. Comparing the deduced drift with the behavior of the magnetic perturbations produced an unexpected result, however, in that the electrojet indicated a positive zonal electric field while the F region drift above it indicated a negative zonal electric field during the same time period. The surprise lies in the fact that the zonal field is usually thought to be quite uniform from the lower E region all the way up to 1000 km. This is related to the normal Sq, which, during the middle of the day, reveals a very consistent current pattern as far as 20 degrees away from the magnetic equator, with a relatively uniform zonal electric field

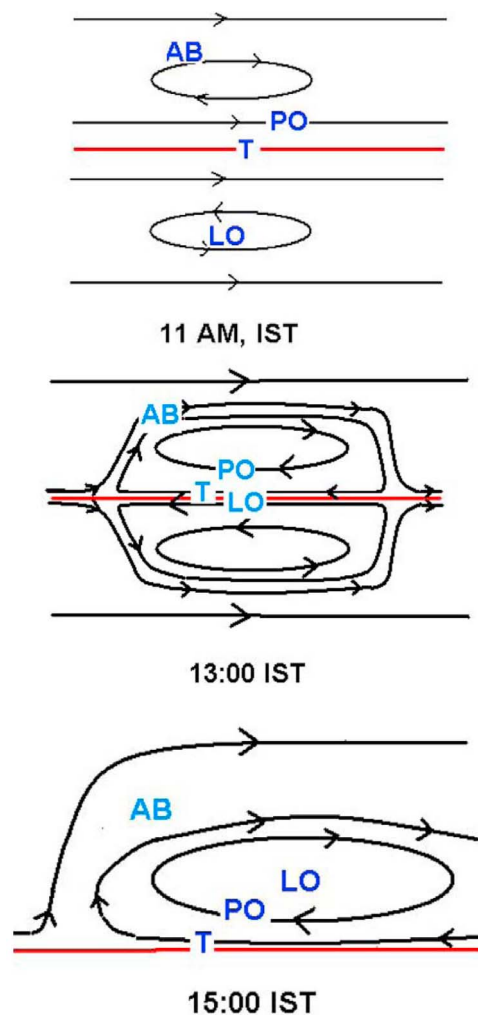


Figure 7. Cartoon to illustrate the competition between the LO-induced clockwise northern current loop and the background normal Sq current pattern. In the 11:00 IST UT plot, the LO is 8 degrees to the south of the magnetic equator and the associated current does not have to close at the equator. In the 13:00 IST plot, the low is centered on the magnetic equator. In the 15:00 IST plot, the LO is to the northeast of Trivandrum. Also shown are the approximate locations of the LO and of the Trivandrum-Tirunelveli and Alibagh stations. The magnetic equator is shown by the transverse red line.

(beyond those latitudes, of course, the current finally turns around to complete its loop).

[41] One point that should be clear, however, is that there is no fundamental physics that requires the zonal electric field in the middle of the day to be unstructured between the magnetic equator and 20° latitude. Indeed, *Blanc and Richmond* [1980] have shown that when thermospheric wind patterns are modified by strong high latitude Joule heating during magnetic storms, a dominant westward wind pattern could be generated at low latitudes, with a very different Sq current pattern that could even turn the EEJ into a CEJ under the right set of circumstances. This phenomenon has been observed repeatedly on days that followed

intense magnetic storms [e.g., *Scherliess and Fejer*, 1997; *Le Huy and Amory-Mazaudier*, 2005, and references therein]. Likewise, *St.-Maurice et al.* [2011] have argued that through the introduction of an anomalous LO at its center, an eclipse passing near the magnetic equator should produce similar tendencies resulting into a weakening or reversal of the EEJ current.

[42] In both instances (disturbance dynamo, and eclipse), the anomalous westward currents and underlying westward zonal electric fields are primarily situated near the equator. Somewhere at higher latitudes, however, the currents should be stronger than normal, since the current loop induced by a LO or by a wide daytime region of westward winds has to close poleward of the LO or poleward of the westward wind region. This would explain why around the time of the eclipse the Sq current values are one standard deviation above average, 10 degrees north of the equator and beyond (see Figure 3). To help visualize this point and other points in the rest of this discussion, we have produced a cartoon of the local equatorial electrojet region in Figure 7, inspired by a somewhat similar diagram by *St.-Maurice et al.* [2011]. In the '11 AM' plot, we illustrate how the position and strength of the LO would be such that Alibagh, 10 degrees to the north, would see an enhancement over normal Sq current values.

[43] The fact that between 10:00 IST and 12:00 IST the F region drift was indicative of a westward zonal field while the EEJ data indicated an eastward field meant that a reversal in the electric field and currents had to take place between the equator and a few degrees poleward of the equator. While this was taking place, furthermore, the EEJ was gradually weakening, until the temporary increase due to noon PRE mentioned earlier. The weakening started when the ionosonde data showed that latitudes a few degrees poleward of the equator (altitudes less than 300 km at the equator) already were under the influence of a westward field. As illustrated in the '11 AM' plot of Figure 7, this means that the influence of the LO, which was centered approximately 8 degrees to the south of the magnetic equator at the time, was not strong enough to reverse the currents at the magnetic equator. That is to say, the LO was far enough from the magnetic equator to have the associated current loop close mostly away from the equator while the normal Sq current trend at the equator could still be seen.

[44] From the moment the eclipse passed over the magnetic equator (13:00 IST plot in Figure 7), a strong CEJ became manifest, as seen in the Tirunelveli magnetometer data after 13:00 IST. Thus, from 12:15 IST onwards, the signs of the F region vertical drift and of the electrojet currents matched one another (1PM plot in Figure 7). The match was complete with a change in the sign of the vertical drift back to normal taking place around 16:15 IST and a change in the sign of the currents occurring some time past 17:00 IST (given that the precise point at which the zero crossing took place depended, for the slowly changing conditions, on knowing ΔH with a precision better than 5 nT, we consider this later comparison to be in very good agreement). Consistent with this, the Pondicherry magnetometer data, just poleward of the electrojet (Figure 3) also indicated a weak reversal in the sign of the electric field in the early afternoon hours.

[45] There remain two important questions, namely, (1) why did the electrojet weaken without changing sign in the late morning hours while the F region above it had already undergone an electric field reversal? and (2) why was there a clear contrast with the afternoon hours, when the electrojet simply reversed its direction? Again using Figure 7 as a guide, the explanation should be that the electric field at the equator was weakening due to the influence of the LO and its local 'counter-Sq' current loop was being felt. However, between 10 and 12 LT, the LO had to compete with the relatively strong normal Sq system formed at that time of day (linear superposition of two opposite processes, 11 AM plot in Figure 7). A few degrees away from the magnetic equator, but not at the magnetic equator itself, the influence of the LO was apparently just strong enough to introduce a reversal in the zonal field (explaining the occurrence of weak downward plasma drifts below 300 km at the equator). At the time the eclipse crossed the magnetic equator (13:00 IST plot in Figure 7), its currents had to close through the equator so that the LO produced its strongest equatorial perturbations for the day. Later on, in the afternoon, after the LO had crossed the magnetic equator (15:00 IST plot in Figure 7), its influence was stronger only 'by default', since the normal Sq current and its effect on the EEJ is always much weaker at that time of day. This would in turn explain the asymmetry between morning and afternoon hours, that is, a weakened but un-reversed EEJ in the morning with weak downward F region drifts, compared to a strong CEJ in the afternoon with stronger downward F region drifts.

4. Conclusion

[46] The annular eclipse of January 15, 2010, over the magnetic equator in Trivandrum, India, produced a traveling low pressure system (LO) centered on the region of maximum obscuration. North of the magnetic equator this LO was at the center of local clockwise current loop immersed into the larger scale counter-clockwise current loop associated with the normal Sq current system. As the LO approached the magnetic equator in the late morning hours, it first weakened the equatorial electrojet without changing its sign. However, the F region, closer to the center of the LO, did show evidence for a zonal electric field reversal through a weak downward plasma drift. In the afternoon hours, the influence of the LO became much larger from the moment the eclipsed region crossed the magnetic equator, around the local noon hours. From that moment on, the clockwise current loop associated with the LO had a much stronger influence on the system because, if nothing else, the normal Sq is much weaker in the afternoon than in the morning hours.

[47] A reversal in the zonal electric field accompanied the reversal in the current direction between the equator and latitudes equatorward of the LO. The ionosonde data show that, except for one hour around noon when a 'pre-reversal-enhancement' associated with the accumulation of negative charges near the eastward terminator of the eclipse, the F region vertical drift below 350 km was downward after 10:00 IST. A first consequence of this prolonged period of downward drift was a relative depletion in the Vertical Total Electron Content (VTEC) at the magnetic equator over Trivandrum, particularly in the early afternoon hours, when

the downward drift was pushing the plasma in a region where recombination was becoming important. In turn, the lack of an upward drift from the main photo-production region near 300 km (where recombination becomes negligible) implied that the Equatorial Ionization Anomaly (EIA) was largely cut off from its normal plasma supply from equatorial/very low latitudes. This meant a substantial depletion in the VTEC not just near the magnetic equator itself, but also all the way to Bhopal, 14.5 degrees north of the magnetic equator. In other words, through electro-dynamical effects, the eclipse influenced the density of a region that was much wider than could have been anticipated from obscuration factors alone. In fact, the effect on the EIA started before the eclipse reached the region and ended well after the eclipse had moved away.

[48] **Acknowledgments.** TEC measurements from GPS were carried out under a coordinated program, GPS Aided Geo Augmented Navigation (GAGAN), jointly operated by the Indian Space Research Organization (ISRO) and the Airport Authority of India (AAI). We acknowledge World Data Center for Geomagnetism, Kyoto for 1 min symH data. The authors thank both referees for their very useful comments and K. Krishnamoorthy and T. K. Pant for useful discussions. J.-P.S.-M. gratefully acknowledges an ADCOS fellowship from the ISRO.

[49] Robert Lysak thanks R. Sridharan and Christine Amory for their assistance in evaluating this paper.

References

- Afraimovich, E. L., K. S. Palamartchouk, N. P. Perevalova, V. V. Chernukhov, A. V. Lukhnev, and V. T. Zalutsky (1998), Ionospheric effects of the solar eclipse of March 9, 1997, as deduced from GPS data, *Geophys. Res. Lett.*, *25*, 465–468.
- Altadill, D., J. G. Solé, and E. M. Apostolov (2001), Vertical structure of a gravity wave like oscillation in the ionosphere generated by the solar eclipse of August 11, 1999, *J. Geophys. Res.*, *106*, 21,419–21,428.
- Anderson, D. N. (1973), A theoretical study of the ionospheric F region equatorial anomaly—I. Theory, *Planet. Space Sci.*, *21*, 409–419.
- Blanc, M., and A. D. Richmond (1980), The ionospheric disturbance dynamo, *J. Geophys. Res.*, *85*, 1669–1686.
- Chimonas, G., and C. O. Hines (1970), Atmospheric gravity waves induced by a solar eclipse, *J. Geophys. Res.*, *75*, 875.
- Cohen, E. A. (1984), The study of the effect of solar eclipse on the ionosphere based on satellite beacon observations, *Radio Sci.*, *19*, 769–777.
- Eccles, J. V. (1998), Modeling investigation of the evening prereversal enhancement of the zonal electric field in the equatorial ionosphere, *J. Geophys. Res.*, *103*, 26,709–26,719.
- Farley, D. T., E. Bonelli, B. G. Fejer, and M. F. Larsen (1986), The prereversal enhancement of the zonal electric field in the equatorial ionosphere, *J. Geophys. Res.*, *91*, 13,723–13,728.
- Fejer, B. G., and L. Scherliess (1997), Empirical models of storm time equatorial zonal electric fields, *J. Geophys. Res.*, *102*, 24,047–24,056, doi:10.1029/97JA02164.
- Greenspan, M. E., C. E. Rasmussen, W. J. Burke, and M. A. Abdu (1991), Equatorial density depletions observed at 840 km during the great magnetic storm of March 1989, *J. Geophys. Res.*, *96*, 13,931–13,942.
- Hanson, W. B., and R. J. Moffett (1966), Ionization transport effects in the equatorial F region, *J. Geophys. Res.*, *71*, 5559–5572.
- Kelley, M. C. (1989), *The Earth's Ionosphere*, Int. Geophys. Ser., vol. 43, Academic, San Diego, Calif.
- Kutiev, I., P. Marinov, A. Belehaki, B. Reinisch, and N. Jakowski (2009), Reconstruction of topside density profile by using the topside sounder model profiler and digisonde data, *Adv. Space Res.*, *43*, 1683–1687.
- Lee, C.-C., and B. W. Reinisch (2007), Quiet-condition variations in the scale height at F2-layer peak at Jicamarca during solar minimum and maximum, *Ann. Geophys.*, *25*(12), 2541–2550.
- Le Huy, M., and C. Amory-Mazaudier (2005), Magnetic signature of the ionospheric disturbance dynamo at equatorial latitudes: "D_{dyn}," *J. Geophys. Res.*, *110*, A10301, doi:10.1029/2004JA010578.
- Müller-Wodarg, I. C. F., A. D. Aylward, and M. Lockwood (1998), Effects of a mid-latitude solar eclipse on the thermosphere and ionosphere—A modelling study, *Geophys. Res. Lett.*, *25*, 3787–3790.
- Nair, K. N., R. G. Rastogi, and V. Sarabhai (1970), Daily variation of the geomagnetic field at the dip equator, *Nature*, *226*, 740–741.

- Rastogi, R. G., and J. A. Klobuchar (1990), Ionospheric electron content within the equatorial F_2 layer anomaly belt, *J. Geophys. Res.*, *95*, 19,045–19,052.
- Ratcliffe, J. A. (1956), A survey of solar eclipses and the ionosphere, in *Solar Eclipses and the Ionosphere*, edited by W. J. G. Beynon and G. M. Brown, pp.1–13, Pergamon, London.
- Reddy, C. A., and C. V. Devasia (1973), Formation of blanketing sporadic E-layers at the magnetic equator due to horizontal wind shears, *Planet. Space Sci.*, *21*, 811–812, doi:10.1016/0032-0633(73)90098-6.
- Reinisch, B. W., and X. Huang (2001), Deducing topside profiles and total electron content from bottomside ionograms, *Adv. Space Res.*, *27*, 23–30.
- Rishbeth, H. (1971), Polarization fields produced by winds in the equatorial F-region, *Planet. Space Sci.*, *19*, 357–369.
- Roble, R. G., B. A. Emery, and E. C. Ridley (1986), Ionospheric and thermospheric response over Millstone Hill to the May 30, 1984, annular solar eclipse, *J. Geophys. Res.*, *91*, 1661–1670.
- Scherliess, L., and B. G. Fejer (1997), Storm time dependence of equatorial disturbance dynamo zonal electric fields, *J. Geophys. Res.*, *102*, 24,037–24,046, doi:10.1029/97JA02165.
- Schunk, R. W., and A. F. Nagy (2000), *Ionospheres: Physics, Plasma Physics, and Chemistry*, Cambridge Atmos. Space Sci. Ser., Cambridge Univ. Press, Cambridge, U. K.
- Smith, D. A., E. A. Araujo-Pradere, C. Minter, and T. Fuller-Rowell (2008), A comprehensive evaluation of the errors inherent in the use of a two-dimensional shell for modeling the ionosphere, *Radio Sci.*, *43*, RS6008, doi:10.1029/2007RS003769.
- Sridharan, R., C. V. Devasia, N. Jyoti, D. Tiwari, K. S. Viswanathan, and K. S. V. Subbarao (2002), Effects of solar eclipse on the electrodynamic processes of the equatorial ionosphere: A case study during 11 August 1999 dusk time total solar eclipse over India, *Ann. Geophys.*, *20*, 1977–1985, doi:10.5194/angeo-20-1977-2002.
- St.-Maurice, J. P., and D. G. Torr (1978), Nonthermal rate coefficients in the ionosphere: The reactions of O^+ with N_2 , O_2 , and NO , *J. Geophys. Res.*, *83*, 969–977.
- St.-Maurice, J.-P., K. M. Ambili, and R. K. Choudhary (2011), Local electro-dynamics of a solar eclipse at the magnetic equator in the early afternoon hours, *Geophys. Res. Lett.*, *38*, L04102, doi:10.1029/2010GL046085.
- Tomás, A. T., H. Lühr, M. Förster, S. Rentz, and M. Rother (2007), Observations of the low-latitude solar eclipse on 8 April 2005 by CHAMP, *J. Geophys. Res.*, *112*, A06303, doi:10.1029/2006JA012168.
- Van Zandt, T. E., R. B. Norton, and G. H. Stonehocker (1960), Photochemical rates in the equatorial F_2 region from the 1958 eclipse, *J. Geophys. Res.*, *65*, 2003–2009.
- Zong, Q.-G., B. W. Reinisch, P. Song, Y. Wei, and I. A. Galkin (2010), Day-side ionospheric response to the intense interplanetary shocks–solar wind discontinuities: Observations from the digisonde global ionospheric radio observatory, *J. Geophys. Res.*, *115*, A06304, doi:10.1029/2009JA014796.

K. M. Ambili and R. K. Choudhary, Space Physics Laboratory, VSSC, Trivandrum, Kerala 695022, India. (ambilikm@yahoo.com; rajkumar_choudhary@vssc.gov.in)

B. M. Pathan, Indian Institute of Geomagnetism, New Panvel, Mumbai, Maharashtra 410206, India. (bmpathan@iigs.iigm.res.in)

J.-P. St.-Maurice, Institute for Space and Atmospheric Studies, University of Saskatchewan, 116 Science Pl., Saskatoon, SK S7N 5E2, Canada. (jp.stmaurice@usask.ca)

S. Sunda, GAGAN, Airports Authority of India, Space Applications Centre, Ahmedabad 380015, India. (ssunda@sac.isro.gov.in)